Pharmaceutical Research, Vol. 24, No. 6, June 2007 (© 2007)
DOI: 10.1007/s11095-006-9219-7

Research Paper

Optical Imaging of the Adoptive Transfer of Human Endothelial Cells in Mice Using Anti-Human CD31 Monoclonal Antibody

Alexei A. Bogdanov Jr.,[1,3] Charles P. Lin,[2] and Hye-Won Kang[1]

Received November 1, 2006; accepted December 15, 2006; published online March 21, 2007

Purpose. The development of endothelium-specific imaging agents capable of specific binding to human cells under the conditions of flow for the needs of regenerative medicine and cancer research. The goal of the study was testing the feasibility of optical imaging of human endothelial cells implanted in mice.
Methods. Mouse model of adoptive human endothelial cell transfer was obtained by implanting cells in Matrigel matrix in subcutaneous space (Kang, Torres, Wald, Weissleder, and Bogdanov, Jr., Targeted imaging of human endothelial-specific marker in a model of adoptive cell transfer. Lab. Invest. **86**: 599-609, 2006). Several endothelium-specific proteins were labeled with near-infrared fluorochrome (Cy5.5) and tested *in vitro*. Fluorescence imaging using anti-human CD31 antibody was performed *in vivo*. The obtained results were corroborated by using fluorescence microscopy of tissue sections.
Results. We determined that monoclonal anti-human CD31 antibodies labeled with Cy5.5 were efficiently binding to human endothelial cells and were not subject to rapid endocytosis.We further demonstrated that specific near-infrared optical imaging signal was present only in Matrigel implants seeded with human endothelium cells and was absent from control Matrigel implants. Histology showed staining of cells lining vessels and revealed the formation of branched networks of CD31-positive cells.
Conclusions. Anti-human CD31 antibodies tagged with near-infrared fluorochromes can be used for detection of perfused blood vessels harboring human endothelial cells in animal models of adoptive transfer.

KEY WORDS: adoptive transfer; CD31; endothelium; fluorescence; molecular imaging; near-infrared; PECAM-1.

INTRODUCTION

A variety of endothelium-targeting strategies are currently being evaluated for the needs of imaging of quiescent and proliferating endothelial cells in cancer, inflammation and atherosclerosis (reviewed in (2,3). Among the endothelial-specific cell surface molecules, $\alpha_v\beta_3$ integrin overexpression (4,5), VCAM-1 (6,7) and E-selectin (1,8) were identified as potential targets associated with inflammation and cell activation. Moreover, recent progress in phage display antibody screening enabled organ-specific targeting of endothelium *in vivo* (9).

The expression of CD31 (platelet-endothelial cell adhesion molecule-1, PECAM-1) by endothelial cells is traditionally used for detecting endothelial cells in tissue sections, for example, to obtain microvascular density scores reflecting angiogenesis and anti-angiogenic treatments (10,11). However, the same marker could be used for detecting endothelial cells *in vivo*. We previously observed prominent and lasting staining of endothelial apical surface exposed to blood perfusion using *in vivo* transdermal, confocal imaging (12). Rat anti-mouse CD31 antibodies covalently labeled with Cy5.5 near-infrared fluorochrome showed an abundant staining of the vascular wall after the *in vivo* injection that was still detectable for 24–48 h after the administration. *in vivo* administration of anti-mouse CD31 antibodies had no toxic effects and showed high specificity to mouse endothelial cells.

We further investigated whether non-invasive imaging can be used to track human, rather than mouse endothelial cells *in vivo*. Human endothelial cells support the formation of perfused blood vessels in athymic mice if implanted in extracellular matrix in the presence of heparin and VEGF (1,13). Initially, we developed and performed testing of targeted MRI contrast agents that associate only with human endothelium expressing pro-inflammatory marker E-selectin. The latter was induced by treating cells with IL-1β or TNFα. After showing high affinity and specificity to activated human endothelium *in vitro* (14), we used *in vivo* model that was developed by implanting human umbilical vein endothelial cells (HUVEC) dispersed in Matrigel matrix. After injecting animals with E-selectin targeted iron oxide nanoparticles, we observed a specific change of MRI signal associated with human endothelial cells.

[1] S2-804, Department of Radiology, University of Massachusetts Medical School, 55 Lake Ave North, Worcester, Massachusetts 01655, USA.
[2] Wellman Center for Photomedicine, Massachusetts General Hospital, Boston, Massachusetts, USA.
[3] To whom correspondence should be addressed. (e-mail: Alexei.Bogdanov@umassmed.edu)

We report here an attempt to detect constitutive, rather than inducible expression of human endothelial differentiation marker by using monoclonal anti-human CD31. The choice of CD31 molecule as a target for imaging was based on the following assumptions: (1) CD31 is a marker of endothelial differentiation; (2) the antibody does not cross-react with mouse cells; (3) similar to the previously used H18/7 anti-E-selectin antibody, anti-CD31 antibody has high affinity to the target protein; (4) CD31 is constitutively expressed on the surface of the endothelium; and (5) internalization of this antibody proceeds at a lower rate than that of anti-E-selectin-specific antibodies. We describe here the experiments that supported some of these predictions using a whole body fluorescence imaging approach for detecting human endothelial cell-lined blood vessels in live animals.

EXPERIMENTAL METHODS

Modification of Proteins with Fluorescent Dyes. Thirty-35 nmol of *U. europaeus* or *L. esculentum* lectins (Vector Labs) or anti-human CD31 monoclonal antibody (Centocor Inc., Malvern PA, provided by Dr. Marian Nakada (15), were diluted in 0.2 ml of 0.1 M sodium bicarbonate pH 8.7 and 6 μl Cy5.5-NHS (GE-Healthcare, Piscataway, NJ) at 50 mg/ml DMSO (10:1 molar ratio) were added and incubated for 30 min (Fig. 1). Mouse monoclonal anti-human E-selectin H18/7 $F(ab')_2$ fragments (a generous gift of Dr. Michael Gimbrone, Vascular Research Division, Brigham and Womens' Hospital), rat anti-mouse CD31 (BD Pharmingen) or anti-human CD31 monoclonal antibodies were modified with Alexa Fluor 488-NHS ester (Molecular Probes-Invitrogen) at the same ratio as described above. Labeled proteins were purified by using spin-chromatography on Bio-Spin P30 minicolumns (Bio-Rad, Hercules CA).

Cell Culture. HUVECs were provided by Dr. Bill Luscinskas, (Vascular Research Division, Department of Pathology, Brigham and Women's Hospital) and propagated in 5% FBS, complete endothelial cell growth medium (EGM, Cambrex, Baltimore, MD) until confluent. Mouse cardiac endothelial cells were provided by Dr. Jennifer Allport-Anderson (Center for Molecular Imaging Research, MGH) and maintained in EGM-2MV medium (Cambrex). Cells were plated in the glass-coverslip chambers (Lab-Tek II, Electron Microscopy Sciences, Hatfield PA). Cells were stained with Cy5.5-labeled lectins (5 μg/ml) and then by Alexa Fluor 488-labeled CD31 monoclonal antibodies (10 μg/ml) diluted in 2% serum in Hanks' solution, washed and postfixed in 2% formaldehyde in PBS. Fluorescence images were acquired using Nikon TE2000-U inverted microscope equipped with a 100 W Dia-illuminator and Nikon blue and red excitation fluorescence filter cubes. Images were acquired using CoolSnapHQ-M CCD (Photometrics, Tucson AZ) and processed using IP Lab Spectrum software (BD Biosciences Bioimaging, Rockville MD).

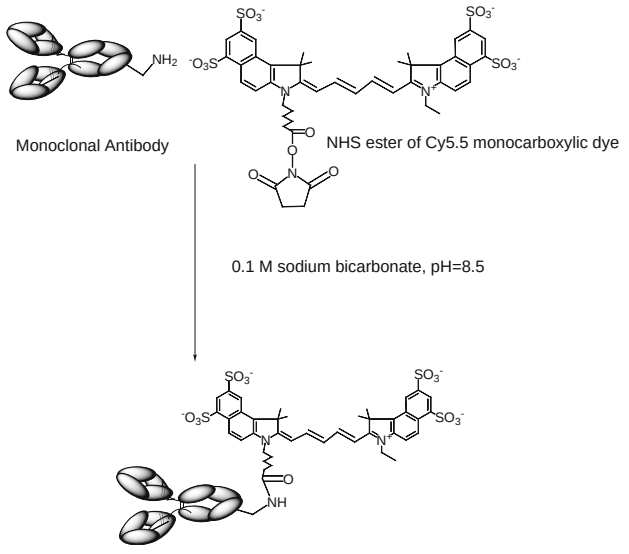

Fig. 1. A schema showing covalent modification of anti-CD31 antibodies with *N*-hydroxysuccinimide ester of Cy5.5 monocarboxylic dye at one of the lysine ε-amino groups of the Fc-fragment.

For confocal microscopy experiments the cells were plated as above, incubated at room temperature with Cy5.5-anti-human CD31 monoclonal antibody and anti-human E-selectin (H18/7) $F(ab')_2$ antibody fragments labeled with Alexa Fluor 488 (10 μg/ml), followed by washing with Hanks' balanced salts saline. Near-infrared fluorescence was excited using HeNe laser (at 633 nm), Alexa Fluor fluorescence was excited using titanium:sapphire laser (at 820 nm) in two-photon excitation mode (12,16).

Matrigel Implantations in Mice. All animal experiments below were approved by UMASS Institutional Animal Care and Use Committee. Injections of HUVEC suspensions in growth-factor-supplemented Matrigel matrix (BD Sciences, Bedford, MA) was performed as described in (1). Briefly, female *nu/nu* mice (Charles River, Stone Ridge NY), 20–25 g, were anesthetized by intraperitoneal injection of a mixture of Ketamine (80 mg/kg) and Xylazine (12 mg/kg) and flank subcutaneous injections were performed by using tuberculin syringe with a hypodermic needle (27 G), Matrigel mixed with HUVECs or Matrigel alone (0.6–0.8 ml) was injected into the right and left posterior flanks of mice, respectively.

Optical Imaging. Mice ($n = 3$, chosen from a group of eight with minimal Matrigel volume decrease, 30 d after the implantation) bearing HUVEC-containing and contralateral control Matrigel implants were anesthetized as described above and injected I.V. with 50 μg of anti-human CD31 monoclonal antibody (approx. 0.7 nmol of conjugated Cy5.5). The animals were imaged immediately and 3 h post implantation using Xenogen IVIS100 (XFO-12 fluorescence imaging option, Xenogen, Hopkinton MA). Exposure times were 1–5 s using Cy5.5 background-corrected excitation filter. Fluorescence was quantitated by using ROI method applied to Live Image (Xenogen) software-generated radiance maps (17).

RESULTS

Testing of Fluorescent-labeled Lectins as Endothelial Markers. The comparative testing of lectins that have *N*-acetylglucosamine and alpha-L-fucose specificities (from tomato and *Ulex europaeus*, respectively) was performed in cultures of HUVEC and mouse vascular endothelial cells

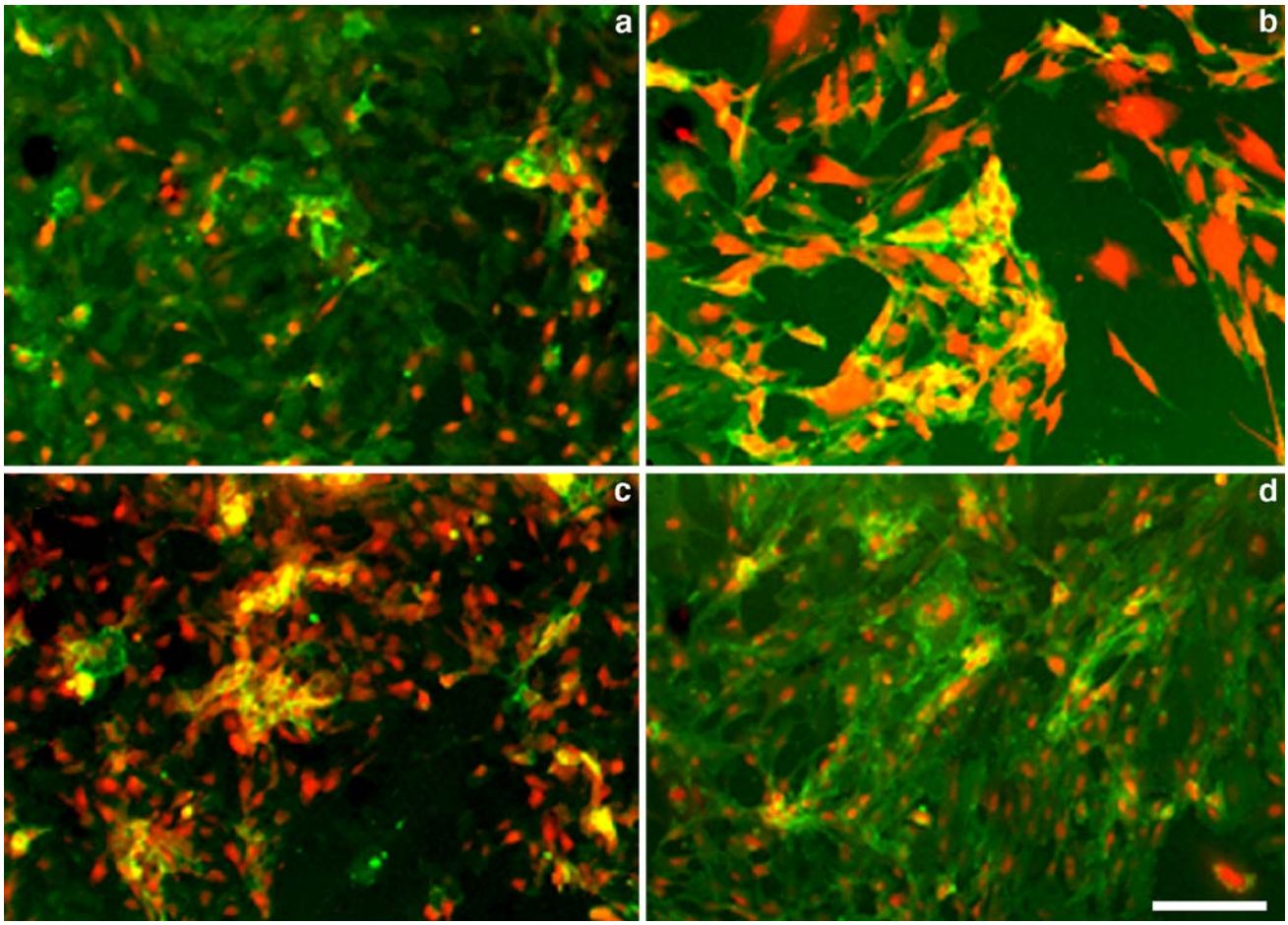

Fig. 2. Fluorescence microscopy of lectin- and anti-CD31 antibody stained human (HUVEC, **a**, **c**) and mouse (lung **b**, **d**) endothelial cells. **a**, **b** cells were stained with Cy5.5-labeled tomato (*L. esculentum*), lectin (at 5 μg/ml, *shown in red*) and Alexa Fluor 488-labeled CD31 monoclonal antibody (1 μg/ml, *shown in green*); **c**, **d** cells were stained with Cy5.5-labeled *U. europaeus* lectin (*L. esculentum*), lectin (5 μg/ml, *shown in red*) and Alexa Fluor 488-labeled CD31 monoclonal antibody (1 μg/ml, *shown in green*). Anti-CD31 antibodies were species-specific. Bar= 50 μm.

(MVEC). Double staining with Cy5.5-labeled lectins and specific monoclonal anti-CD31 antibodies showed that near-infrared dye conjugated lectins were efficiently binding to the surface of endothelial cells (Fig. 2, red). As expected, *Ulex* lectin showed bright staining of human endothelial cells, whereas tomato lectin resulted in prominent fluorescence in MVEC cultures. However, in both HUVEC and MVEC cultures the specificity of these lectins was insufficient since cross-reactivity of both lectins was present, i.e., human cells showed binding of tomato lectin and mouse cells were positively stained with *Ulex* lectin. In both cases, species-specific anti-CD31 antibodies showed homogenous staining (Fig. 2, green) suggesting that the cultures of primary endothelial cells were pure and did not contain contaminating cells that could potentially result in a biased lectin binding.

Antibody Binding and Internalization. In Vitro Two Photon, Confocal Imaging of HUVECs. Double staining of live HUVEC cells with Cy5.5-conjugated anti-human CD31 and Alexa Fluor 488 conjugated anti E-selectin (CD62E) antibody revealed high levels of near-infrared signal (anti-CD31 antibody) associated with intracellular junctions and apical plasma membrane surface but little binding of the labeled anti-E-selectin antibody. After treating cells with IL-1β we observed binding and partial internalization of CD31 (Fig. 3, staining of cell surface and partial staining of intracellular vesicles, color coded in red). Anti-E-selectin antibody fragments were efficiently internalized resulting in staining of intracellular vesicles (shown green-color coded) while no plasma membrane fluorescence was detectable. Internalization was completely blocked by *N*-ethylmaleimide (50 μM) and by incubating cells at 4°C (not shown). In the latter case, fluorescence-labeled anti-E-selectin antibody was rapidly internalized after transferring cultures to room temperature.

Imaging of HUVEC in Matrigel Implants In Vivo. Mice with HUVEC seeded in Matrigel and implanted via a subcutaneous injection were kept for 3–4 weeks before imaging to establish human cell-lined blood vessels. At this time point the volume of injected Matrigel "implants" decreased approximately 50% as a result of partial degradation. HUVEC-seeded Matrigel implants usually showed slower degradation/absorption than the control implants. Intravenous injection of 50 μg Cy5.5-labeled anti-human CD31 antibody resulted in a progressive increase of the average mouse body fluorescence signal over the first 5 min

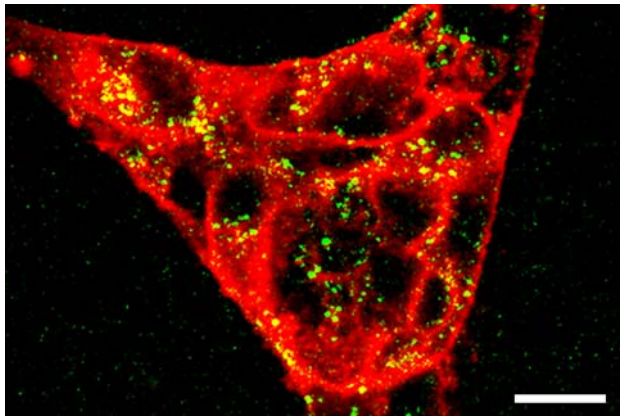

Fig. 3. Immunofluorescent confocal and two photon microscopy showing IL-1β treated HUVEC stained with: *red*—anti-human CD31, labeled with Cy5.5, fluorescence excited with HeNe laser (at 633 nm); *green*—anti-human E-selectin monoclonal antibody (H18/7) F(ab')$_2$ fragments labeled with Alexa Fluor 488. Fluorescence excited using titanium:sapphire laser (at 820 nm) in two-photon excitation mode. Bar=20 μm

after the injection, which was followed by a gradual removal of the imaging probe from the circulation. Approximately 2.5 h after the injection the normalized signal/noise ratios were in the range of 1.6–2. These ratios were measured assuming a diffuse fluorescence source within the mouse and by using average radiances, i.e., the normalized directional photon fluxes from the measured ROI areas. The difference in observed radiances resulted in HUVEC-implant/background tissue ratios that provided sufficient implant/tissue contrast in lateral images (right lateral, Fig. 4a, arrow). Conversely, control implants were indistinguishable from the background tissue (left lateral, Fig. 4b, arrow). However, the uptake of a fraction of the labeled Cy5.5-antibody in the spleen showed a signal in the midline of the body in left lateral projection image (Fig. 4b). The spleen was visible due to the close proximity of the spleen to the surface of the mouse body and potential elevated uptake of antibody aggregates. The comparative measurements (expressed as average radiance) performed using region-of-interest selected over the HUVEC/Matrigel implants and control Matrigel implants showed an average 1.6–1.8—times increase of radiance that was easily discernible on the near-infrared images (Fig. 4c).

Immunofluorescent Histology of Matrigel Implants. We analyzed Matrigel frozen sections obtained from mice that were preinjected with Cy5.5-labeled anti-human CD31 antibody. Using near-infrared emission filter we observed structures that traced the shape of endothelium-lined vessels (Fig. 5a). These elongated positively stained structures were absent in HUVEC-free control Matrigel implants. The staining of sections harvested from mice that were not injected with fluorescent antibody was used to visualize cell nuclei (DAPI, blue, Fig. 5a and b) and CD31 endothelium-specific marker (mouse or human). Using triple staining with Cy5.5-anti-human CD31 antibody (Fig 5b, red), Alexa Fluor 488-labeled anti-mouse CD31 antibody (green) and DAPI staining, we observed a branched vascular network that was almost entirely positive for human marker and negative for mouse marker (Fig. 5b). Some areas on stained sections

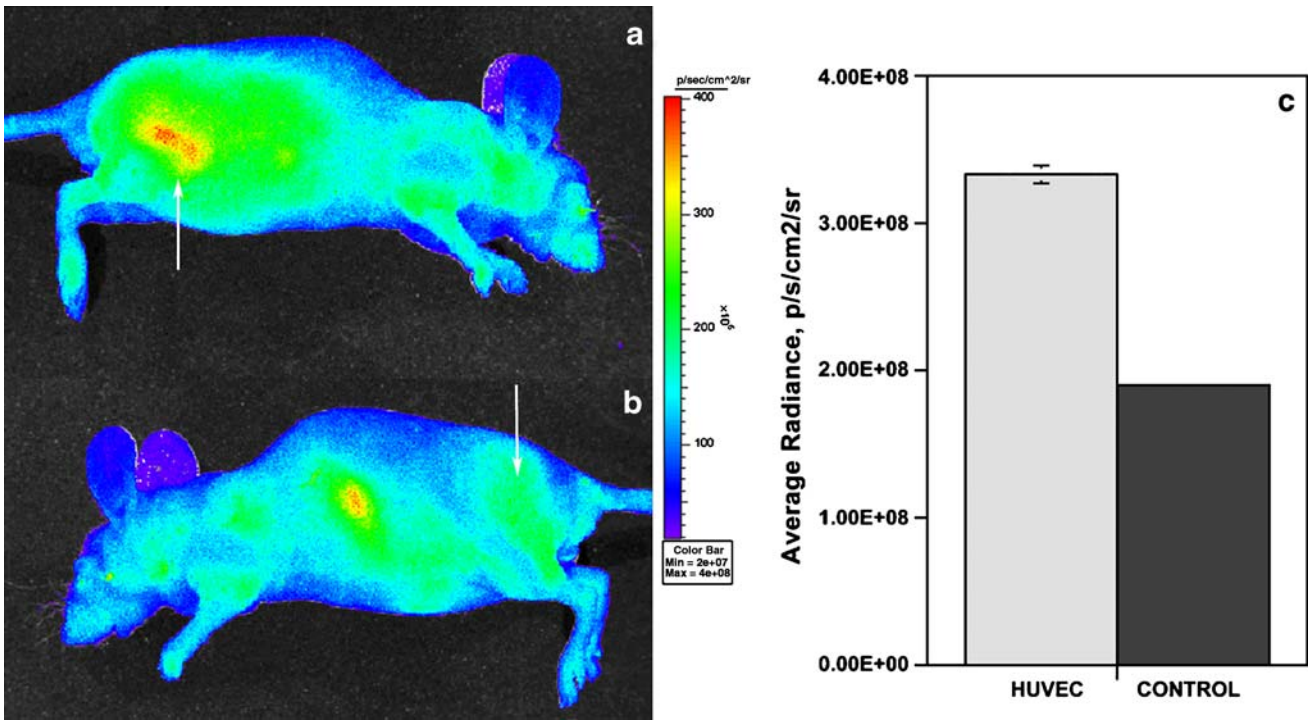

Fig. 4. Representative fluorescent *in vivo* imaging of a mouse injected with 50 μg Cy5.5-labeled anti-human CD31 antibody using Xenogen IVIS100 (XFO-12 fluorescence imaging option). **a** lateral image of a mouse with HUVEC-containing Matrigel implant (*shown by an arrow*); **b** lateral image of the same mouse with a control implant (*shown by an arrow*). Pseudocolor image showing scaled radiance values is layered over a visible light image. *Color scale is shown on the right.* **c** average radiance measured over four non-overlapping ROI (area—3 mm^2) in HUVEC-containing and control implants (mean ± SD, $n=3$). Fluorescence excited using background correction and collected in 695–770 nm range.

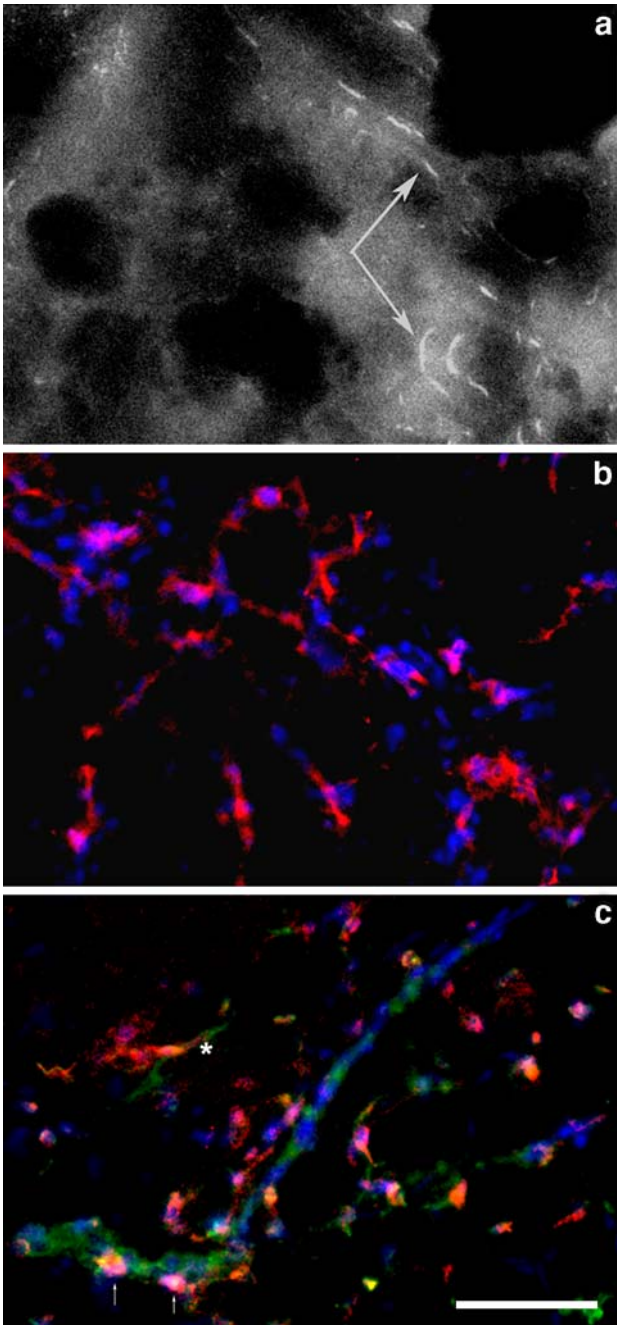

Fig. 5. Fluorescence microscopy of HUVEC-containing Matrigel implants (frozen sections). **a** Cy5.5 fluorescence in implants removed from imaged mice. Arrows point to fluorescent-labeled vessel lining cells. **b** staining of HUVEC-implants with Cy5.5-labeled anti-human CD31 (*red*) and DAPI (*blue*). **c** staining of HUVEC-implants with Cy5.5-labeled anti-human CD31 (*red*), Alexa Fluor 488-labeled anti-mouse CD31 antibody (*green*) and DAPI. The *asterisk* indicates a mouse-human vessel junction; the *arrows* show human endothelial cells incorporated in mouse vessel. Bar = 100 μm.

showed mouse blood vessels that usually contained none or very few human CD31-positive cells (Fig. 5c, human cells shown with arrows). Human-positive blood vessels existed mainly as independent networks with a very few "mosaic" engrafted mouse-CD31 positive cells. Some human vessels appeared to have junctional connectivity with mouse vessels, which manifested in 1–2 discernible "green–red" transitions per section (Fig. 5c, asterisk).

DISCUSSION

Engineering of "humanized" blood vessels using pure isolates of human endothelial cells is a potential alternative to grafting of human skin for propagating human blood vessels in immunocompromised rodents (13,18–20). The need of *in vivo* model systems that utilize functional human blood-perfused vessels is dictated by the needs of anti-angiogenic therapies development as well as the needs of tissue engineering in regenerative medicine. Vascular non-invasive imaging could serve as an important adjunct to monitoring of the fate of cell adoption and eventual acceptance *in vivo*. Imaging offers a strategy for testing and selecting potential imaging agents directed at the human-specific endothelial target molecules. In particular, imaging of fluorescence in the near-infrared range is especially useful for detecting receptor–ligand or enzyme–substrate interactions in subcutaneous implants due to the fact that near-infrared light has lower scattering and is less absorbed by tissues and blood *in vivo* (21,22). Moreover, recent progress in development of quantitative methods in optical imaging, resulted in feasibility of fluorescence tomography *in vivo*, which enables three-dimensional reconstruction of fluorescence sources and allows measurements of fluorochrome concentrations (23,24).

We (1) and others (19) previously reported the formation of blood vessels in VEGF and FGF-2 supplemented Matrigel extracellular matrix mixed with human endothelial cells. Matrigel has an important advantage of a natural cell adhesion matrix (collagen I and laminin-based extracellular matrix) in that it exists in a fluid state at lower temperatures and rapidly solidifies at mouse body temperatures *in vivo*. It has been previously reported that Matrigel supports sprouting and stabilization of microvessels (25,26). Human endothelial vessels generated in mice using collagen implants were found to be immature, transient and having a tendency to regress (13). However, 4–6 week survival time span of HUVEC-lined vessels was sufficient for our experiments, limited only by continuing degradation and absorption of Matrigel matrix.

We initially tested lectins with well-established endothelial specificity to determine whether they could assist in differentiating between human and mouse endothelial cells. For example, the ability of *N*-acetylglucosamine-specific tomato lectin to bind to the apical surface of mouse endothelial cells is well known; and the injection of mice with relatively low amounts of this protein (20–50 μg/animal) enables visualization of tumor blood vessels (27,28). We compared tomato lectin with lectin from *U. europaeus* which has specificity for fucosylated molecules on human endothelium (29). Both lectins showed high sensitivity to endothelial cell surface glycoproteins. However, binding experiments in endothelial cell culture demonstrated that both tomato and *Ulex* lectins did not exhibit sufficiently high specificity and showed cross-reactivity with human and mouse endothelial cells, respectively. Therefore, we chose to investigate whether human endothelial cells *in vivo* could be imaged by using mouse monoclonal antibodies generated against human

CD31 chimeric protein (15). These antibodies demonstrated high levels of binding to constitutively expressed CD31 and resulted in specific association with human endothelial cells (Fig. 2, green fluorescence). Unlike human-E-selectin, which is rapidly internalized and degraded (30,31), CD31 adhesion molecule surface expression is not triggered by pro-inflammatory stimuli and is less extensively internalized by endothelial cells after specific antibody binding (Fig. 3). This suggests human CD31 as an attractive target for *in vivo* imaging. We tested this by using *in vivo* imaging (Fig. 4) and *ex vivo* histology (Fig. 5). The presence of high imaging signal in HUVEC-seeded Matrigel implants and bright staining of vessel-lining cells suggested the presence of intact and viable human endothelial cells in animals at 30 days after the implantation. The observed high target/background imaging signal contrast suggested that the anti-human CD31 antibodies showed no cross-reactivity with mouse endothelial lining cells and suggested no leakage from mouse neovessels formed in Matrigel *in vivo*. The observed uptake of antibodies in the spleen of mice was supposedly a result of labeled antibody aggregation with potential opsonization in plasma, and could be viewed as a limitation of the method. However, the use of antibody fragments instead of the whole antibody and the removal of aggregates using sedimentation of size-exclusion methods are expected to decrease the non-specific uptake in non-target organs. Histology suggested that mouse and human vascular networks co-exist predominantly as parallel structures. However, several points of human blood vessel branching off mouse vessels were present and visible by using labeling histology sections with anti-human and anti-mouse CD31 antibodies (Fig. 5b, c).

It is remarkable that human CD31-positive cells (Fig. 5b) appear to be surrounded by many mouse cells (CD31 negative, DAPI stain positive). We are currently investigating whether this is a result of the recruitment of mouse supporting (mural) cells in response to FGF-2. This could explain an unusual longevity of the human blood vessels in mice that survive for 6 weeks without any additional exogenous supporting cell implantation.

In conclusion, we determined that near-infrared fluorescent anti-human CD31 antibodies show promise *in vivo* as a potential imaging agent that could be applied for imaging of adoptive transfer of human endothelial cells in mice. The use of these antibodies could assist in determining the fate of human cells for bioengineering purposes and in drug development.

ACKNOWLEDGEMENTS

This work was supported in part by NIH RO1 EB000858 and EB000664. The authors are grateful to Dr. Marian Nakada (Centocor) for supplying anti-human CD31 monoclonal antibody and to Dr. Bill Luscinskas (Brigham and Women's Hospital) for providing HUVEC cells.

REFERENCES

1. H. W. Kang, D. Torres, L. Wald, R. Weissleder, and A. A. Bogdanov Jr. Targeted imaging of human endothelial-specific marker in a model of adoptive cell transfer. *Lab. Invest.* **86**:599–609 (2006).
2. A. L. Klibanov. Microbubble contrast agents: targeted ultrasound imaging and ultrasound-assisted drug-delivery applications. *Invest. Radiol.* **41**:354–362 (2006).
3. F. G. Blankenberg, C. Mari, and H. W. Strauss. Development of radiocontrast agents for vascular imaging: progress to date. *Am. J. Cardiovasc. Drugs* **2**:357–365 (2002).
4. X. Chen, M. Tohme, R. Park, Y. Hou, J. R. Bading, and P. S. Conti. Micro-PET imaging of alphavbeta3-integrin expression with 18F-labeled dimeric RGD peptide. *Mol. Imag.* **3**:96–104 (2004).
5. H. Leong-Poi, J. Christiansen, A. L. Klibanov, S. Kaul, and J. R. Lindner. Noninvasive assessment of angiogenesis by ultrasound and microbubbles targeted to alpha(v)-integrins. *Circulation* **107**:455–460 (2003).
6. M. M. Sadeghi, J. S. Schechner, S. Krassilnikova, A. A. Gharaei, J. Zhang, N. Kirkiles-Smith, A. J. Sinusas, B. L. Zaret, and J. R. Bender. Vascular cell adhesion molecule-1-targeted detection of endothelial activation in human microvasculature. *Transplant. Proc.* **36**:1585–1591 (2004).
7. K. A. Kelly, J. R. Allport, A. Tsourkas, V. R. Shinde-Patil, L. Josephson, and R. Weissleder. Detection of vascular adhesion molecule-1 expression using a novel multimodal nanoparticle. *Circ. Res.* **96**:327–336 (2005).
8. S. Boutry, C. Burtea, S. Laurent, G. Toubeau, L. Vander Elst, and R. N. Muller. Magnetic resonance imaging of inflammation with a specific selectin-targeted contrast agent. *Magn. Reson. Med.* **53**:800–807 (2005).
9. P. Valadon, J. D. Garnett, J. E. Testa, M. Bauerle, P. Oh, and J. E. Schnitzer. Screening phage display libraries for organ-specific vascular immunotargeting *in vivo*. *Proc. Natl. Acad. Sci. USA* **103**:407–12 (2006).
10. E. R. Horak, R. Leek, N. Klenk, S. LeJeune, K. Smith, N. Stuart, M. Greenall, K. Stepniewska, and A. L. Harris. Angiogenesis, assessed by platelet/endothelial cell adhesion molecule antibodies, as indicator of node metastases and survival in breast cancer. *Lancet* **340**:1120–1124 (1992).
11. S. B. Fox, K. C. Gatter, R. Bicknell, J. J. Going, P. Stanton, T. G. Cooke, and A. L. Harris. Relationship of endothelial cell proliferation to tumor vascularity in human breast cancer. *Cancer Res.* **53**:4161–4163 (1993).
12. J. M. Runnels, P. Zamiri, J. A. Spencer, I. Veilleux, X. Wei, A. Bogdanov, and C. P. Lin. Imaging molecular expression on vascular endothelial cells by *in vivo* immunofluorescence microscopy. *Mol. Imag.* **5**:31–40 (2006).
13. N. Koike, D. Fukumura, O. Gralla, P. Au, J. S. Schechner, and R. K. Jain. Tissue engineering: creation of long-lasting blood vessels. *Nature* **428**:138–139 (2004).
14. H. W. Kang, L. Josephson, A. Petrovsky, R. Weissleder, and A. Bogdanov, Jr. Magnetic resonance imaging of inducible E-selectin expression in human endothelial cell culture. *Bioconj. Chem.* **13**:122–127 (2002).
15. M. T. Nakada, K. Amin, M. Christofidou-Solomidou, C. D. O'Brien, J. Sun, I. Gurubhagavatula, G. A. Heavner, A. H. Taylor, C. Paddock, Q. H. Sun, J. L. Zehnder, P. J. Newman, S. M. Albelda, and H. M. DeLisser. Antibodies against the first Ig-like domain of human platelet endothelial cell adhesion molecule-1 (PECAM-1) that inhibit PECAM-1-dependent homophilic adhesion block *in vivo* neutrophil recruitment. *J. Immunol.* **164**:452–462 (2000).
16. A. Bogdanov Jr., C. Lin, M. Simonova, L. Matuszewski, and R. Weissleder. Cellular activation of the self-quenched fluorescent reporter probe in tumor microenvironment. *Neoplasia* **4**:228–236 (2002).
17. T. Troy, D. Jekic-McMullen, L. Sambucetti, and B. Rice. Quantitative comparison of the sensitivity of detection of fluorescent and bioluminescent reporters in animal models. *Mol. Imag.* **3**:19–23 (2004).
18. J. S. Schechner, A. K. Nath, L. Zheng, M. S. Kluger, C. C. Hughes, M. R. Sierra-Honigmann, M. I. Lorber, G. Tellides, M. Kashgarian, A. L. Bothwell, and J. S. Pober. *In Vivo* formation of complex microvessels lined by human endothelial cells in an immunodeficient mouse. [see comment]. *Proc. Natl. Acad. Sci. USA* **97**:9191–9196 (2000).

19. D. K. Skovseth, T. Yamanaka, P. Brandtzaeg, E. C. Butcher, and G. Haraldsen. Vascular morphogenesis and differentiation after adoptive transfer of human endothelial cells to immunodeficient mice. *Am. J. Pathol.* **160**:1629–1637 (2002).
20. D. R. Enis, B. R. Shepherd, Y. Wang, A. Qasim, C. M. Shanahan, P. L. Weissberg, M. Kashgarian, J. S. Pober, and J. S. Schechner. Induction, differentiation, and remodeling of blood vessels after transplantation of Bcl-2-transduced endothelial cells. *Proc. Natl. Acad. Sci. USA* **102**:425–430 (2005).
21. D. Hawryszand and E. Sevick-Muraca. Developments toward diagnostic breast cancer imaging using near-infrared optical measurements and fluorescent contrast agents. *Neoplasia* **2**: 388–417 (2000).
22. V. Ntziachristos, C. Bremer, and R. Weissleder. Fluorescence imaging with near-infrared light: new technological advances that enable *in vivo* molecular imaging. *Eur. Radiol.* **13**:195–208 (2003).
23. V. Ntziachristos. Fluorescence molecular imaging. *Annu. Rev. Biomed. Eng.* **8**:1–33 (2006).
24. K. Lichaand and C. Olbrich. Optical imaging in drug discovery and diagnostic applications. *Adv. Drug Deliv. Rev.* **57**:1087–1108 (2005).
25. R. F. Nicosiaand and A. Ottinetti. Modulation of microvascular growth and morphogenesis by reconstituted basement membrane gel in three-dimensional cultures of rat aorta: a comparative study of angiogenesis in matrigel, collagen, fibrin, and plasma clot. *In Vitro Cell. Dev. Biol.* **26**:119–128 (1990).
26. A. Passaniti, R. M. Taylor, R. Pili, Y. Guo, P. V. Long, J. A. Haney, R. R. Pauly, D. S. Grant, and G. R. Martin. A simple, quantitative method for assessing angiogenesis and antiangiogenic agents using reconstituted basement membrane, heparin, and fibroblast growth factor. *Lab. Invest.* **67**:519–528 (1992).
27. A. Petrovsky, E. Schellenberger, L. Josephson, R. Weissleder, and A. Bogdanov Jr.. Near-infrared fluorescent imaging of tumor apoptosis. *Cancer Res.* **63**:1936–1942 (2003).
28. D. M. McDonaldand and P. L. Choyke. Imaging of angiogenesis: from microscope to clinic. *Nat Med.* **9**:713–725 (2003).
29. H. Holthofer, I. Virtanen, A. L. Kariniemi, M. Hormia, E. Linder, and A. Miettinen. *Ulex europaeus* I lectin as a marker for vascular endothelium in human tissues. *Lab. Invest.* **47**:60–66 (1982).
30. E. J. von Asmuth, E. F. Smeets, L. A. Ginsel, J. J. Onderwater, J. F. Leeuwenberg, and W. A. Buurman. Evidence for endocytosis of E-selectin in human endothelial cells. *Eur. J. Immunol.* **22**:2519–2526 (1992).
31. P. I. Chuang, B. A. Young, R. R. Thiagarajan, C. Cornejo, R. K. Winn, and J. M. Harlan. Cytoplasmic domain of E-selectin contains a non-tyrosine endocytosis signal. *J. Biol. Chem.* **272**:24813–24818 (1997).